SAG CONFERENCE
VANCOUVER 2015

USING PISTON PRESS TESTS FOR DETERMINING OPTIMAL ENERGY INPUT FOR AN HPGR OPERATION

*Z. Davaanyam[1], B. Klein[1], and S. Nadolski[2]

[1]*Norman B. Keevil Institute of Mining, University of British Columbia*
517-6350 Stores Road,
Vancouver, BC, Canada V6T 1Z4
*(*Corresponding author: zorig@alumni.ubc.ca)*

USING PISTON PRESS TESTS FOR DETERMINING OPTIMAL ENERGY INPUT FOR AN HPGR OPERATION

ABSTRACT

Multiple trade-off studies have shown that grinding circuits with high pressure grinding rolls (HPGR) can be more energy efficient than the circuits with semi-autogeneous (SAG) mills. However, such studies are difficult to conduct because the current practice of sizing and selecting the HPGR requires large samples for pilot-scale testing that are expensive and difficult to obtain. There is therefore a need for a small scale test procedure that can reliably predict the energy requirements of the HPGR for a given ore-body.

Three methodologies involving piston press tests were developed recently at the Norman B. Keevil (NBK) Institute of Mining:

1. The "Direct Calibration Methodology" calibrates piston press test results to pilot-scale HPGR results on a representative composite sample from a deposit. Piston press tests can then be used to determine the energy–size reduction relationship for a range ore types within the deposit.
2. Similarly, the "Database-Calibrated Methodology" calibrates piston press tests against a database of pilot-scale HPGR and piston press tests. The database includes results from pilot scale HPGR tests on 15 different ores for which piston press testing was also conducted.
3. The "Simulation Methodology" involves piston press testing on five narrow size classes of particles at three energy levels from a mineral deposit. The results are used to define the energy–breakage relationship that can be used for circuit simulation.

All three test methods are valuable tools for predicting the energy-size reduction relationship for the HPGR. The ability to conduct simple piston press tests requiring less than 10 kg of sample greatly assists assessment of the HPGR for early stage projects.

KEYWORDS

HPGR, comminution, energy, piston press test, particle breakage, simulation

INTRODUCTION

HPGRs have been shown to be a more energy efficient comminution technology than SAG mills for preparing feed to ball mills. This greater energy efficiency has been reported in many trade-off studies as shown in Table 1. However, the comparison of energy efficiencies of the two technologies can only be determined from testing programs. The current practice of sizing and selecting the HPGR involves pilot-scale testing on 1 to 10 tonne samples, depending on the level of the study. These large samples can be difficult to obtain and the cost of sample collection and pilot scale testing can be prohibitive, particularly for early stage projects.

Thus, the large sample requirement for the pilot-scale HPGR test program remains one of the major barriers to giving a full and fair consideration to HPGR-based comminution circuits. To address this issue, three small scale piston press test procedures were developed at NBK Institute of Mining. The program to develop the tests was supported by the Canadian Mining Industry Research Organization (CAMIRO) and its member companies.

Table 1 – Direct specific energy comparison between SABC and HPGR circuits

Project name	Units	SABC	HPGR	Energy savings [%]	Reference
Boddington Gold	kWh/t	23.10	18.00	22.1	(Parker, Rowe, Lane, & Morrell, 2001)
Los Broncos Copper	kWh/t	16.21	13.02	19.7	(Oestreicher & Spollen, 2006)
Cerro Verde Copper	kWh/t	20.10	15.90	20.9	(Vanderbeek, Linde, Brack, & Marsden, 2006)
Ruby Creek Moly	$/t	4.53	3.83	15.5	(Anguelov, Ghaffari, & Alexander, 2008)
Copper Gold project in Russia	$/t	0.78	0.53	32.1	(Anguelov et al., 2008)
Courageous Lake Gold	$/t	3.59	2.47	31.2	(Anguelov et al., 2008)
Morrison Copper/Gold/Moly	$/t	0.63	0.56	11.1	(Anguelov et al., 2008)
Mine A	kWh/t	19.90	16.90	15.1	(Daniel, Lane, & McLean, 2010)
Mine B	kWh/t	14.80	12.30	16.9	(Daniel et al., 2010)
Mine C	kWh/t	11.10	8.90	19.8	(Daniel et al., 2010)
Case A	kWh/t	14.73	11.03	25.1	(Rosario, 2011)
Case B	kWh/t	15.73	10.73	31.8	(Rosario, 2011)
Ajax Copper/Gold	$/t	0.60	0.47	21.7	(Ghaffari, Anguelov, & Alexander, 2013)
Case H (160 micron grind)	kWh/t	18.76	13.23	29.5	(Wang, 2013)
Case H (75 micron grind)	kWh/t	22.28	18.74	15.9	(Wang, 2013)

EXPERIMENTAL PROCEDURE

Two separate experimental procedures were used to acquire data for use in comparing the methodologies:

Pilot-Scale HPGR Test Work

A Koeppern HPGR unit with 750 mm diameter and 220 mm wide rolls was used for the pilot-scale testing. The ore samples were stage crushed to -32 mm and homogenized using rotary splitter, prior to splitting into 250-350 kg portions (depending on the bulk density) for pilot scale testing. During the homogenization process two representative sub-samples (10–15 kg) were obtained. One sub-sample was used for determining the particle size distribution (PSD), moisture content, and bulk density and the other sub-sample was used for piston press testing.

A data-logger connected to the HPGR was used to record roll speed, torque, power draw and operating gap. Figure 1 shows an example of recorded machine data. When the 250-350 kg feed sample is released from the feed hopper, the power draw (blue line) spikes and hydraulic pressure (green line) fluctuates as the operating gap (red line) expands from the initial static gap of 9 mm. Product samples from the centre and edge were collected for about 20 seconds after the operation stabilized.

The recorded machine data and weights of collected samples were used to calculate net specific energy consumption and specific throughput constant (m-dot) values. The centre and edge product samples were sampled using a rotary splitter and then subjected to sieve analysis to determine the PSDs.

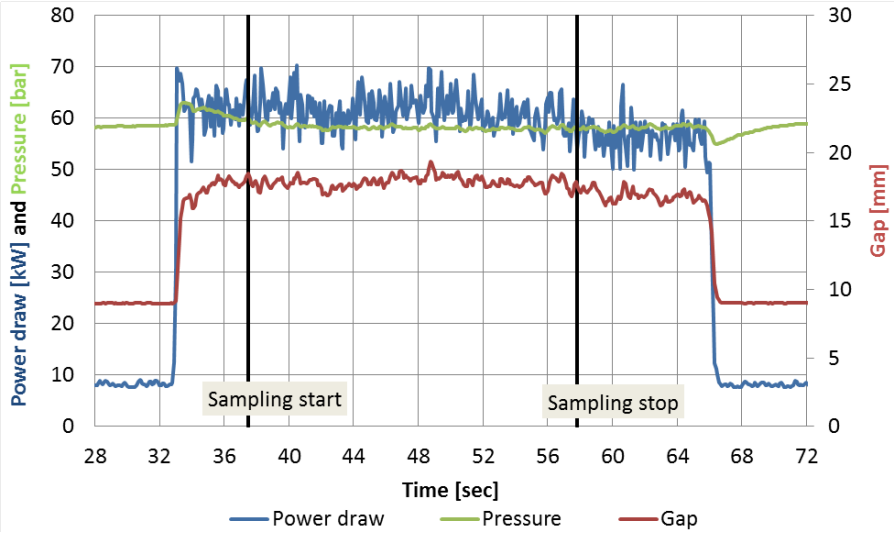

Figure 1 – An example of recorded machine data for an HPGR test

Piston Press Testing

Samples for piston press testing were prepared by stage crushing to -12.5 mm. For each piston press test, a 240 cc volume of sample was weighed and placed in 86 mm hardened steel die. The sample was then pressed with a piston in a hydraulic press as illustrated in Figure 2. The piston position was set to zero at the rim of the die and prior to starting the test, a seating load of 2.5 kN is applied. The piston load was then ramp up at a rate of 200kN/min and the force-displacement readings were logged at 0.25 second time intervals.

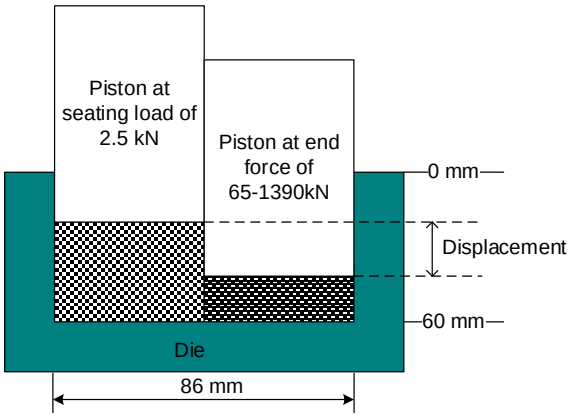

Figure 2 – Illustration of piston-die arrangement

The force–displacement data recorded during the test was corrected for strain within the piston die assembly. An example of force-displacement curve is shown in Figure 3. The strain-corrected force-displacement data was then numerically integrated to determine the total mechanical energy input to the sample. The specific energy was determined by dividing the total energy by the sample weight. The pressed sample was removed from the die by removing the base plate and the product was wet and dry sieved to determine the product PSD.

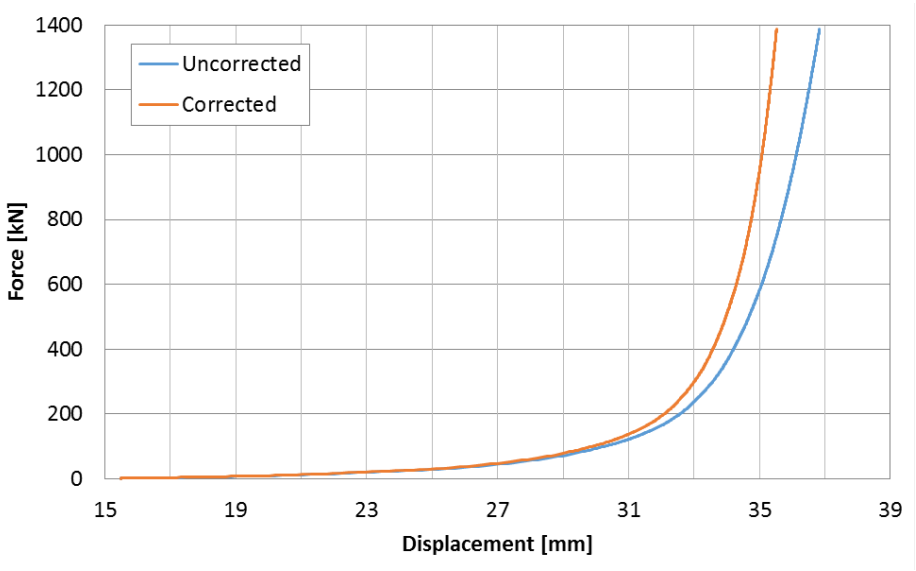

Figure 3 – An example of force-displacement curve before and after the strain correction

RESULTS AND DISCUSSION

Three methods are discussed below for predicting energy-size reduction relationships for HPGRs.

Direct Calibration Methodology

Calibrating piston pressure against specific pressing force

In the Direct Calibration Methodology, the results of piston press tests are calibrated to results from pilot scale HPGR test results to develop a model. The calibrated model can then be used by conducting piston press tests on a range of samples from the deposit to predict variations in the HPGR energy-size reduction relationship.

The specific pressing force, which is the total hydraulic force divided by roll diameter and width, has units of N/mm^2. It is the most important operating parameter and directly influences net specific energy consumption. For the piston press, the piston pressure is determined by dividing the pressing force the area of the piston-die area apparatus. Over the specific pressing force range of 2 to 6 N/mm^2, the net specific energy consumption increases linearly with pressing force. Figure 4 shows the fitted regression lines for net specific energy versus specific pressing force (red line) and piston pressure (blue line). As shown in the graph, a HPGR specific pressing force of 4 N/mm^2 is equivalent a piston pressure of 190 MPa, which both deliver specific energy of 2.0 kWh/t to the tested sample.

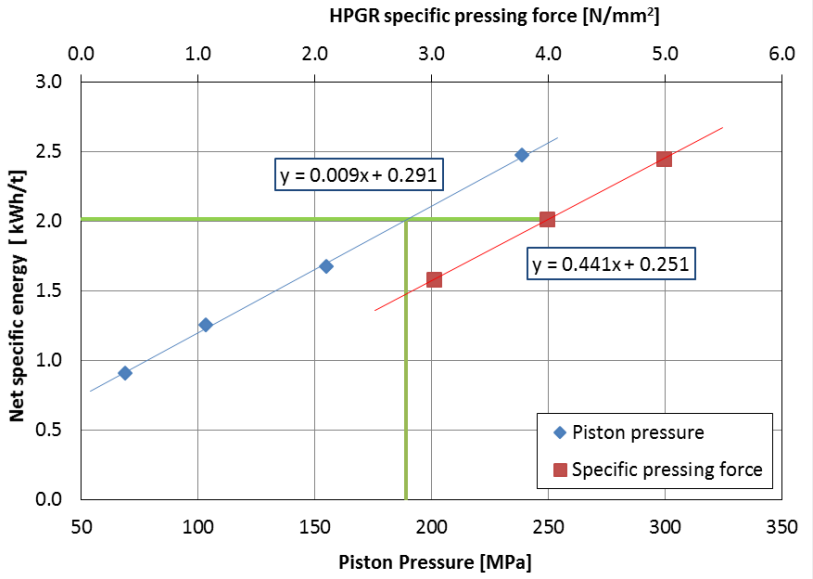

Figure 4 – Illustration of calibration between specific pressing force and piston pressure, such that both deliver the same net specific energy to the sample

The fitted regression equations can be used to calculate the equivalent piston pressure required to deliver the same net specific energy for any given specific pressing force. The generic formula relating piston press pressure, P_{piston}, to HPGR specific pressing force, F_{SP}, is derived in equations 1 to 4.

$$E_{SP} = m_1 \cdot P_{piston} + b_1 \quad (1)$$

$$E_{SP} = m_2 \cdot F_{SP} + b_2 \quad (2)$$

$$m_1 \cdot P_{piston} + b_1 = m_2 \cdot F_{SP} + b_2 \quad (3)$$

$$P_{piston} = \frac{m_2}{m_1} \cdot F_{SP} + \frac{b_2 - b_1}{m_1} \quad (4)$$

Where E_{sp} is the specific energy, P_{piston} is piston pressure, F_{sp} is specific pressing force and m_1, m_2, b_1, b_2 are fitted coefficients. The calibrated model, equation 4, can be defined by the slope (m_2/m_1) and the y-intercept, which is equal to (b_2-b_1)/m_1. In this manner the direct calibration methodology was applied to 15 different ore types and the ore-specific calibration equations for piston press pressure against the specific pressing forces were determined.

Specific Energy Prediction with Piston Press Test

For the direct calibration methodology, it is proposed to develop the calibrated model for a composite sample. The piston press test can then be conducted for a range of samples at appropriate pressing forces to assess variability in specific energy across a mineral deposit. Figure 5 compares the net specific energy for HPGR tests to those predicted from piston press tests. All predictions lie within ±10% envelope. This is considered reasonable for scoping and pre-feasibility level studies.

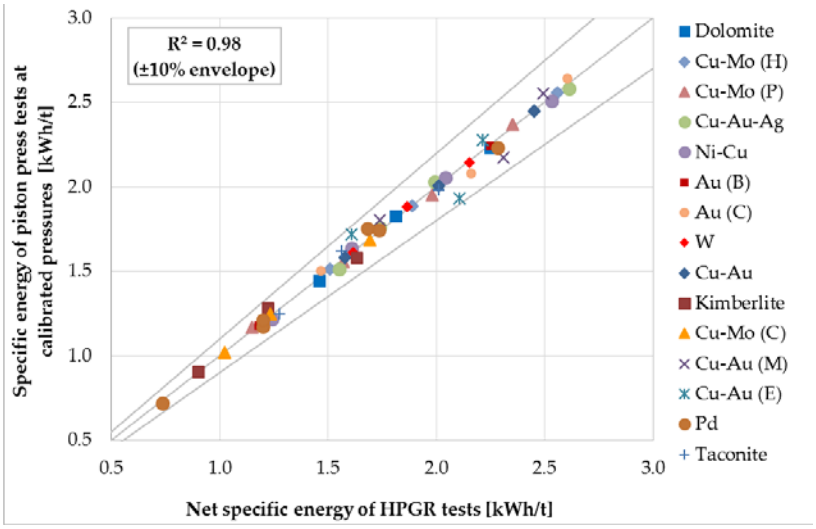

Figure 5 – Specific energy prediction using ore-specific calibration between piston press pressure and specific pressing force

Scaling Size Reduction Achieved in Piston Press Tests

In order to predict the HPGR PSD, the reduction ratio (F50/P50) achieved in piston press is calibrated against the reduction ratio achieved in the HPGR test. While HPGR tests are conducted on -32 mm material, the piston press tests are conducted on -12.5 mm material due to constraints related to the particle size and piston diameter. In order to correlate the data, HPGR tests were also performed on -12.5 mm material. Figure 6 shows the results of HPGR tests performed on -32 mm and -12.5 mm samples. The smaller feed size resulted in a decrease in the reduction ratio is explained as follows:

- The -32 mm feed contains particles that are larger than the operating gap. Therefore, the coarse particles larger than the operating gap are broken with certainty as they pass through the gap, whereas no particle of -12.5 mm feed are broken with certainty.
- Coarser particles have a higher number of flaws or micro-cracks and mineral grain boundaries that can lead to fracture when compared to smaller particles.
- The -12.5 mm feed has a higher proportion of fine particles (e.g. <1 mm), which leads to an isostatic-like state more quickly as compared to the -32 mm feed. Also the fine fractions in the feed approach the behavior of powder, and the probability of breaking fine particles by compression decreases with decreasing particle size.
- Smaller particles are inherently more difficult to break due to the reduced contact area.

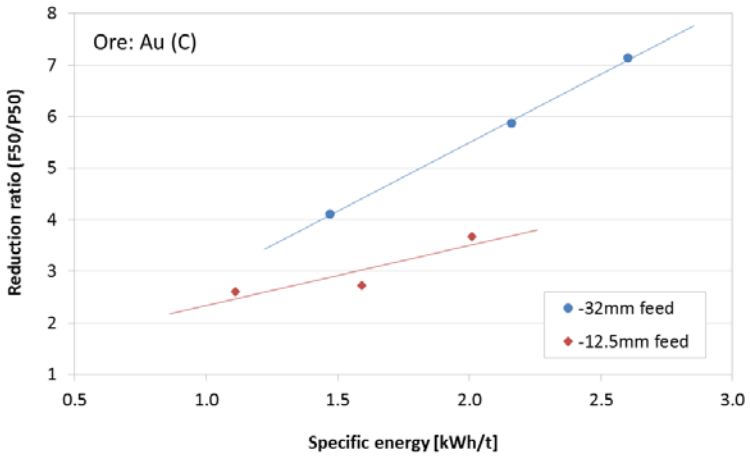

Figure 6 – Comparison of reduction ratios achieved for the HPGR tests on feeds with -32 mm and -12.5 mm feed.

The reduction ratios achieved in the HPGR and the piston press tests can be directly calibrated on the basis of specific energy. The reduction ratio achieved in piston press tests can be modeled using the power law relationship proposed by Norgate and Weller (1994) as shown equation 5.

$$\frac{F_{50}}{P_{50}} = k \cdot E^{b} + 1 \tag{5}$$

Figure 7 (A) presents an example of reduction ratios achieved in piston press tests modeled by equation 5. The fitted model was used to determine reduction ratios at the same net specific energy as the HPGR tests (the hollow circles). Figure 7 (B) is a plot of the calculated reduction ratios from piston press tests versus reduction ratios from HPGR tests. The fitted regression line represents the calibration equation relating reduction ratios between the HPGR and piston press for the tested ore.

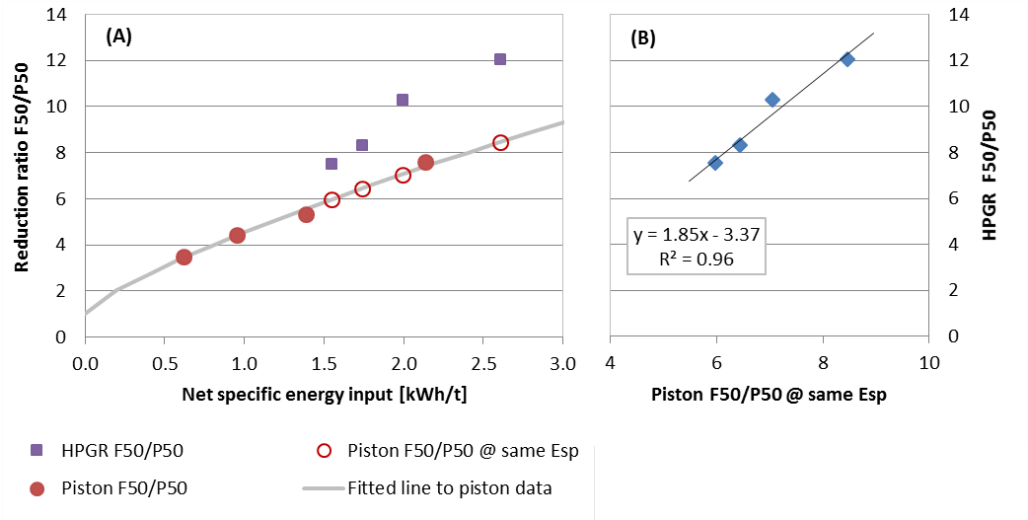

Figure 7 – (A) Reduction ratios from HPGR and piston press tests versus net specific energy and predicted specific energy from piston press tests modelled by equation 5; (B) Calibrated reduction ratio achieved in piston press tests versus the reduction ratios achieved in HPGR tests.

Figure 8 compares the HPGR reduction ratios to the scaled reduction ratios from the piston press tests for 15 different tested ores. The fit of the predicted reduction ratio has a coefficient of determination of 0.98 showing good agreement with those achieved in pilot scale testing.

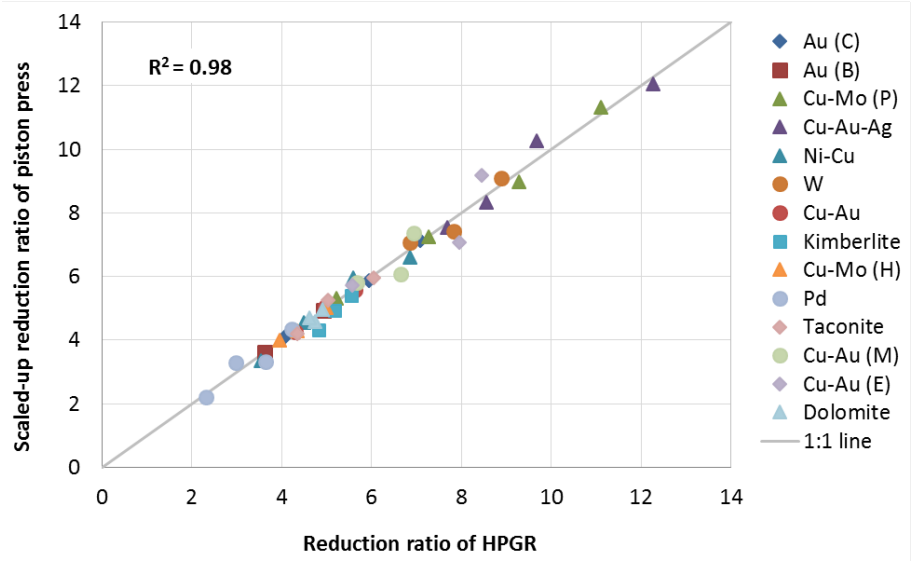

Figure 8 – Comparison of the HPGR reduction ratios with the scaled reduction ratios of the piston press tests

Exploiting Normalized PSDs of Product from Piston Press Test

Both HPGR and piston press tests produce product PSDs that can be normalized by dividing by their median size. Figure 9 (a) shows the PSD for four HPGR test products, conducted at different specific pressing forces. As expected, the highest specific pressing force produced the finest product. When the product PSDs are normalized by dividing by their respective median particle sizes, all four normalized PSDs overlap as shown in Figure 9 (b).

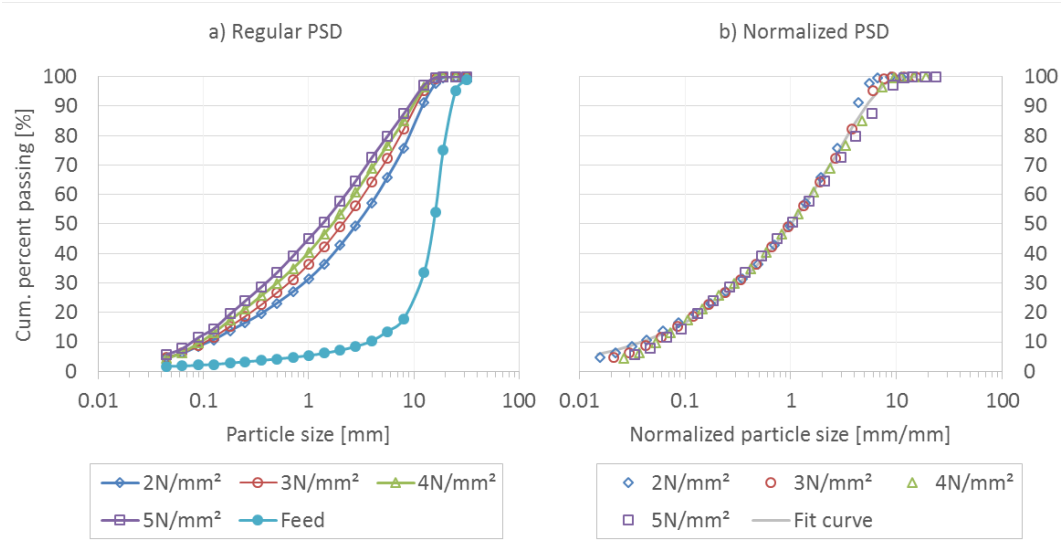

Figure 9 – Comparison of regular product PSDs with normalized product PSDs

The normalized product PSDs can be represented by a single curve. Equation 6 is the functional form of the curve suggested by Lim *et al.* (1996).

$$F\left(\frac{x}{X50}\right) = 100\left(1 - \exp\left(A\left(\frac{x}{X50}\right)^{\left(m\left(\frac{x}{X50}\right)+n\right)}\right)\right) \quad (6)$$

where,
F is cumulative percent passing
x/X50 is the dimensionless particle size normalized by the median size
A, m, and n are fitted parameters.

Figure 10 compares the normalized PSDs of products from HPGR tests on -32 mm and -12.5 mm feed sizes and from piston press tests on -12.5 mm feed. The figure shows that the PSDs match well. The implication of is that normalized product PSDs that have been determined from piston press testing can be used to predict the normalized product PSDs for the HPGR. With the knowledge of the reduction ratio and normalized product PSDs, the full product PSD can be reconstituted.

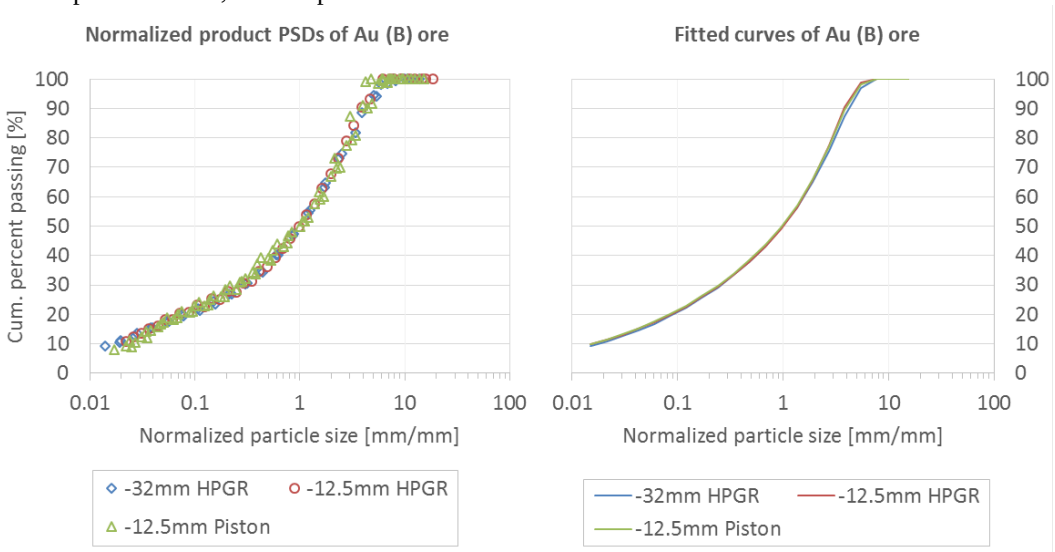

Figure 10 – Comparison of normalized PSDs of products from HPGR tests on -32 mm and -12.5 mm top size feeds and piston press tests on -12.5 mm feed

Summary of the Direct Calibration Methodology

The Direct Calibration methodology can be summarized into the following six steps:

1. Conduct HPGR pilot-scale tests on a composite feed sample.
2. Perform piston press tests on representative sub-sample of the composite feed sample
3. Derive model relating piston press pressure to specific pressing force at the same net specific energy.
4. Calibrate the reduction ratios achieved in the piston press tests to the reduction ratios achieved in HPGR tests on basis of same specific energy.
5. Compare the normalized PSDs of the products from the HPGR tests and piston press tests.
6. Perform piston press tests on various geometallurgical units and scale the piston press test results to predict the HPGR energy-size reduction response.

Figure 11 shows a block diagram of the direct calibration methodology. The methodology requires about 1 tonne of composite sample representing the orebody. The composite sample is used to conduct three pilot-scale HPGR tests and piston press tests at a range of pressures. Once the ore-specific calibrations models are obtained, the models can be used to predict the energy–size reduction information for individual ore types within the deposit.

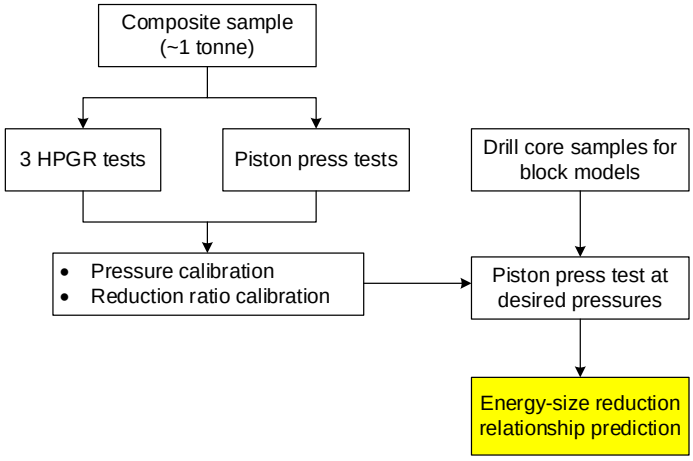

Figure 11 – Block diagram of the direct calibration methodology

Database-Calibrated Methodology

Calculating Piston Pressure Using Empirical Equation

The previously described Direct Calibration Methodology was applied to 15 ore types which generated a data base of 45 pairs of specific pressing force versus piston press pressure data sets. The database was used to develop empirical models to predict the HPGR specific energy and particle size reduction from piston press test results, without the need for pilot-scale HPGR testing.

Equation 7 was generated using multivariable linear regression by fitting piston press pressure to specific pressing force and characteristics of the feed sample.

$$Ppiston = 5.53 + 53.3F_{SP} + 24.3w - 86.2\rho_b + 13.1F_{50}^{H} - 44.4\frac{F_{50}^{H}}{F_{50}^{P}} + 2.98P_{1mm}^{P} \quad (7)$$

where,
P_{piston} is the estimation of required piston pressure in MPa;
F_{SP} is specific pressing force in N/mm^2;
w is moisture content in %;
ρ_b is bulk density in g/cc;
F_{50} are 50% passing feed particle sizes for HPGR and piston press tests;
P_{1mm} is percentage passing 1mm in feed to piston press test.

Figure 12 shows the piston pressure required to deliver the same specific energy into the sample as the HPGR versus the piston pressure calculated using the empirical equation 7. The coefficient of determination R^2 is 0.863 indicating a good fit.

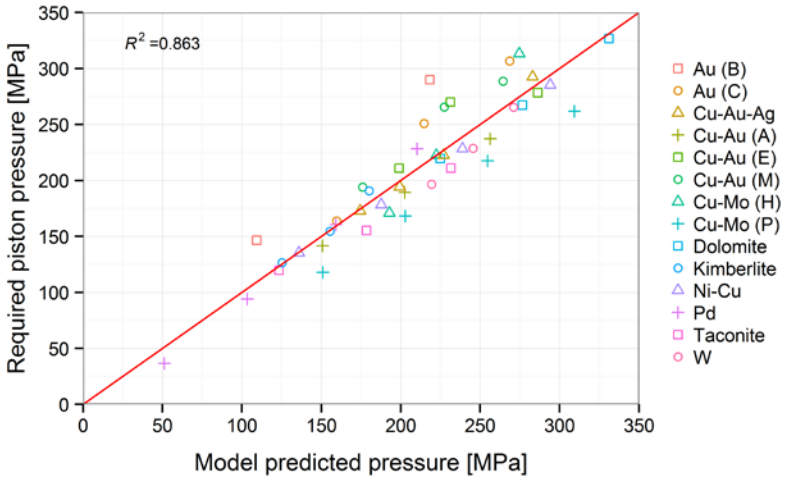

Figure 12 – Required piston pressure to deliver the same specific energy input as the HPGR test versus piston pressure calculated using the empirical equation 7.

Conducting Piston Press Tests at Calculated Pressure

Conducting piston press tests at pressures calculated using the empirical equation 7 and numerical integration of the resulting force-displacement curves provides a prediction of net specific energy of HPGR. Figure 13 shows that the net specific energy predictions are within ±25% of the measured values. This is considered reasonable for scoping level studies.

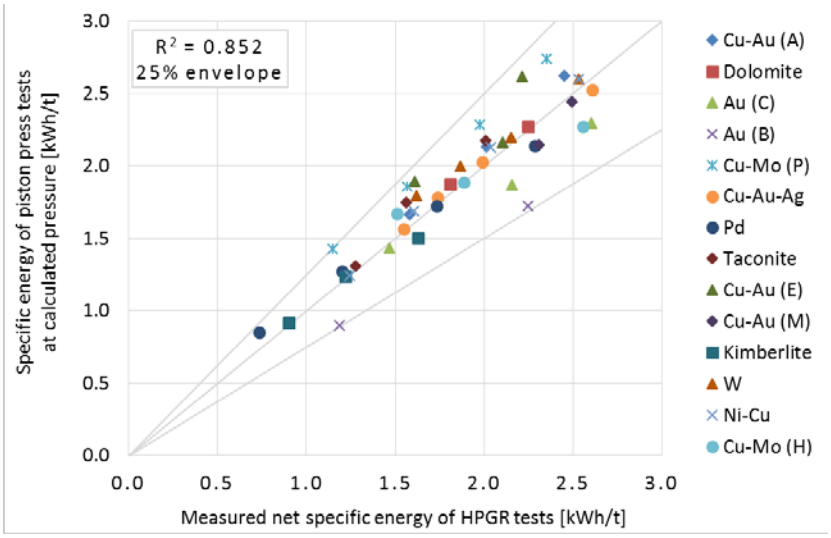

Figure 13 – Predicted net specific energy using equation 7 versus measure values from pilot scale HPGR testing

Scaling Reduction Ratio Using Empirical Equation

The reduction ratios achieved in the piston press test is scaled to that of the HPGR using equation 8.

$$RR_H = 1.86 + 1.41RR_P + 2.31\frac{F_{50}^H}{F_{50}^P} - 0.41F_{50}^H - 1.02w \quad (8)$$

where,
RR_H is the predicted reduction ratio for the HPGR;
RR_P is the reduction ratio achieved in a piston press test;
w is the moisture content of feed;
$F_{50}^{H, P}$ are the 50% passing particle size of the feed to the HPGR (H) and piston press tests (P).

Figure 14 shows the predicted reduction ratio as determined by equation 8 versus those determined from HPGR tests. The coefficient of determination of 0.828 indicates a fit of predicted versus measured responses.

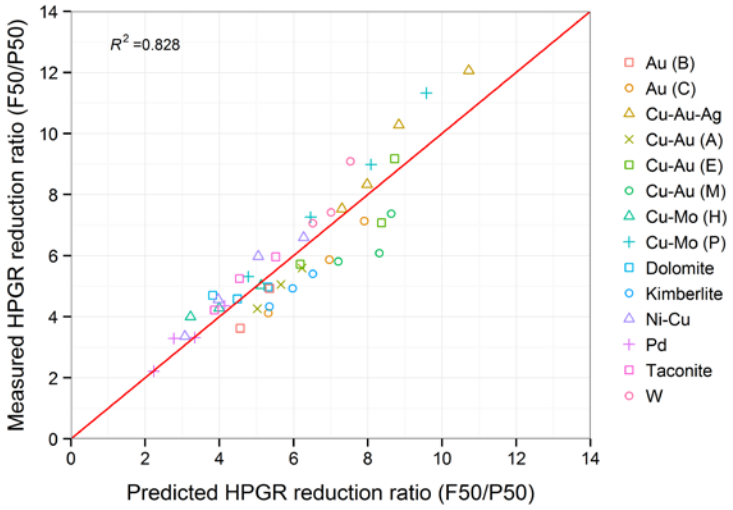

Figure 14 – Measured reduction ratio achieved in HPGR tests versus scaled reduction ratio achieved in piston press test using the empirical equation 8

Summary of the Database-calibrated Methodology

The database-calibrated methodology can be summarized with the following four steps:

1. Calculate the piston press pressure using equation 7. The desired specific pressing force is a variable in the equation.
2. Conduct the piston press tests at the pressures calculated in the step 1.
3. Scale the reduction ratio achieved in piston press tests to that of the HPGR using the empirical equation 8.
4. Predict the energy–size reduction performance of the HPGR assuming the normalized PSDs of products from the piston press and the HPGR tests are the same.

Figure 15 is a block diagram showing the database-calibrated methodology. The database-calibrated methodology has the advantage over the direct calibration methodology in that it requires only piston press testing and does not require large sample for pilot-scale HPGR testing. Rather, equation 7 is used to calculate the piston pressure corresponding to the desired specific pressing force. Then equation 8 is used to scale the reduction ratio achieved in the piston press test to that of the HPGR. The level of

accuracy from of the direct calibration methodology is considered to be greater than the accuracy of the database-calibrated methodology. .

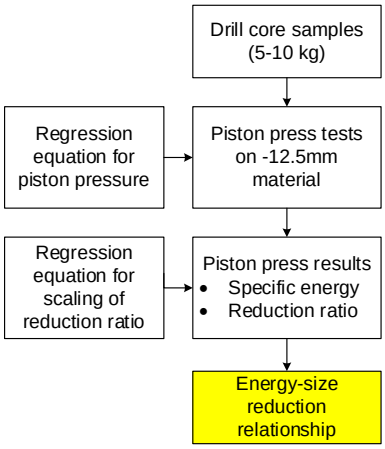

Figure 15 – Block diagram of the database-calibrated methodology

Simulation Methodology

The direct calibration and the database-calibrated methodologies are considered empirical approaches. They require either HPGR test data for calibration or empirical equations obtained from a database to calculate piston pressures and to scale the reduction ratio achieved in piston press tests. These empirical methodologies cannot be used for simulation of closed-circuit operation of HPGR.

The simulation-based methodology is semi-empirical in that the energy–breakage relationship of the ore is characterized by performing piston press tests on particles in narrow size fractions. Then the knowledge of the ore breakage characteristic is used to simulate the energy–size reduction performance for the HPGR.

Defining the Energy–Breakage Relationship for Compression Bed Breakage

For the simulation methodology piston press tests are conducted on multiple classes of narrowly sized particles at three energy levels each. The ore characterization involves compressed bed breakage and is analogous to JK Drop Weight testing which characterizes impact breakage.

Shi and Kojovic (2007) proposed an energy–breakage model (Eq. 9) for impact breakage that incorporates the effect of particle size. The model was modified for compressed bed breakage for application to the HPGR. The addition of exponent *n* to equation 10 was justified because by including the additional parameter, the residual standard error of the model was reduced significantly.

$$t_{10} = M\left(1 - \exp(-f_{mat} \cdot x \cdot E_{SP})\right) \quad (9)$$

$$t_{10} = M\left(1 - \exp(-f^{*}_{mat} \cdot x^{n} \cdot E_{SP})\right) \quad (10)$$

where,

t_{10} is percentage passing 1/10th of the initial particle size and represents the degree of breakage after energy input E_{SP} [%]

M is a fitted parameter and represents the maximum attainable value of t_{10} [%]

f_{mat} is a fitted parameter and represents the material properties [t/kWh·mm^{-n}]

x is particle size [mm]

E_{SP} is specific energy input [kWh/t]

An example of modelling t_{10} with equation 10 is given in Table 2 and plotted in Figure 16 where the fitted curve describes the measured data well.

Table 2 – An example of modelling t_{10} with equation 10

Particle size [mm]	Specific energy [kWh/t]	Measured t_{10} [%]	Modelled t_{10} [%]	Error square
-12.5+11.2	3.14	39.62	37.50	4.46
	1.35	25.15	25.16	0.00
	0.30	7.75	7.66	0.01
-9.5+8.0	3.08	34.79	35.66	0.76
	1.32	22.23	22.84	0.37
	0.40	7.72	8.76	1.08
-6.7+5.6	3.04	33.33	33.42	0.01
	1.30	21.45	20.32	1.27
	0.41	7.21	7.92	0.51
-4.75+4.0	2.95	29.33	30.82	2.22
	1.20	17.16	17.27	0.01
	0.40	7.64	6.81	0.68
-2.8+2.0	2.99	25.29	26.99	2.92
	1.17	16.70	13.80	8.41
	0.43	7.17	5.74	2.05
			Sum of squared error	24.74
			Residual standard error	1.44
			95% prediction interval	3.23

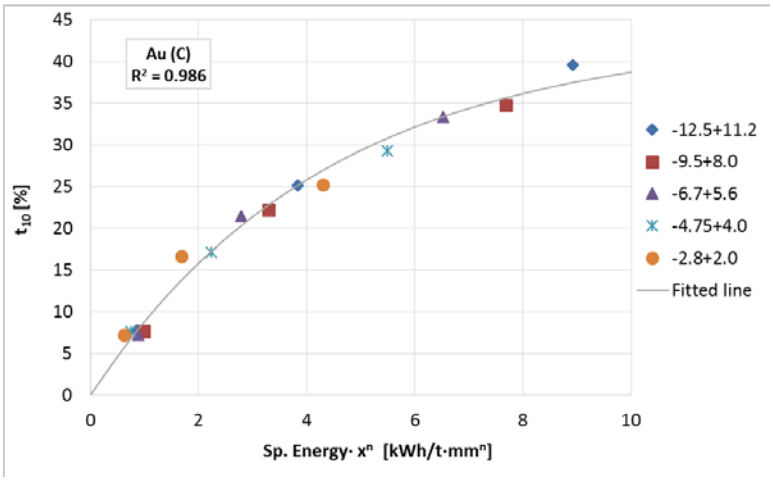

Figure 16 – Measured t_{10} values for piston press tests on a gold ore and the fitted curve

In compression breakage, fine particles are believed to play a role. Since the piston press tests are conducted on narrowly sized particles and there are no fines present, the influence of the presence of fines was quantified by conducting piston press tests on admixture of narrowly sized particles (-12.5 +11.2 mm) and fines (-0.5 mm). The proportion of fines was varied from 0 to 75% by weight. The results showed that equation 11 adequately predicts the t_{10} resulting from piston press tests on admixtures using the same values for M, f^*mat, and n determined through conducting piston press tests on narrowly sized particles. Figure 17 shows the predicted (Eq. 11) versus measured t_{10} values.

$$t_{10} = \left(M - c \cdot P_{fines}\right)\left(1 - \exp\left(-f^*_{mat} \cdot x^n \cdot E_{SP}\right)\right) \quad (11)$$

where, c is a fitted constant to multiply by the percentage of fines in the feed, P_{fines}.

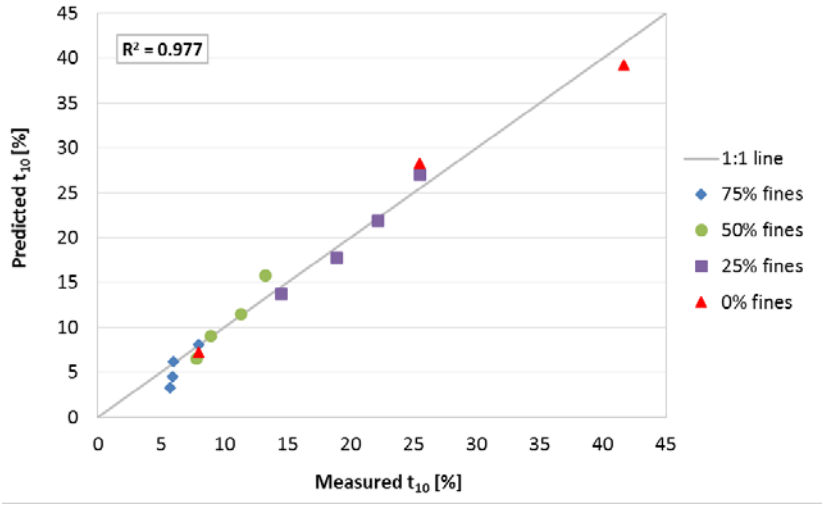

Figure 17 – Predicted versus measured t_{10} resulting from the piston press tests conducted in the presence of fines

Determining the Full Size Distribution of the Progeny Using t_{10}

Other t_n values, which represent the percentage passing $1/n^{th}$ of the initial particle size, can be determined from piston press product PSDs. Plotting t_n against t_{10} suggest that there is a set of master curves that describe the t_{10}–t_n relationships regardless of ore type as shown in Figure 18. Therefore the whole PSD after breakage can be reconstituted with knowledge of t_{10} alone.

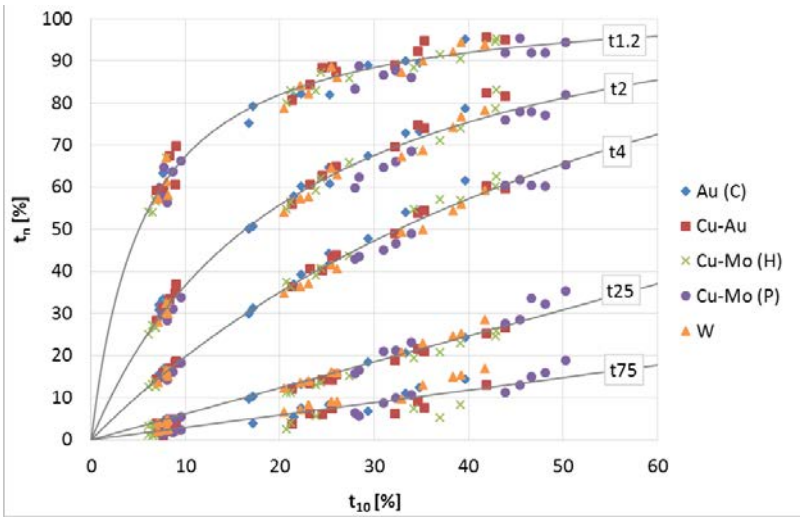

Figure 18 – A set of master curves describing each t_{10}–t_n relationships

Simulation of the Energy–Size Reduction Performance of the HPGR

Once the energy–breakage relationship is defined and the set of master curves describing the t_{10} versus t_n relationship are known, the energy–size reduction performance of the HPGR can be simulated using a spreadsheet software such as Excel.

Figure 19 is a block diagram model showing the simulation methodology. Similar to the Morrell/Tondo model (Morrell, Lim, Shi, & Tondo, 1997), the simulation model assumes that the feed particles are split into two fractions, according to a critical size, x_c. However, the coarser particles in the feed are assumed to break by compressed bed mechanisms rather than by single particle impact breakage. The breakage in the pre-crushing stage can be modeled using equation 10 because the effect of fine particles is assumed minimal.

In the model, the product from the pre-crushing stage is combined with the finer fraction and the combined product is subjected to the grinding stage. In other words, the coarse particles break via both pre-crushing and grinding stages, while the fine particles break only via the grinding stage. The breakage in the grinding stage is modeled by equation 11 because when the particle bed is fully compacted the presence of fines significantly affects the interparticle breakage.

The total energy is distributed between the pre-crushing and the grinding stages. The energy to the pre-crushing stage is assumed to be a function of the fraction of coarser particles in the feed as shown in equation 12 and the specific energy in the pre-crushing stage is calculated using equation 13.

$$E^{crush} = \beta_{split} \cdot f_{coarse} \cdot E^{total} \quad (12)$$

$$E_{SP}^{crush} = \beta_{split} \cdot E_{SP} \quad (13)$$

where, β_{split} is a model parameter.

The specific energy for the grinding stage is calculated using equation 14 and is the difference between the total energy being simulated and the energy expended in the crushing stage.

$$E_{SP}^{grind} = E_{SP} \cdot (1 - \beta_{split} \cdot f_{coarse}) \quad (14)$$

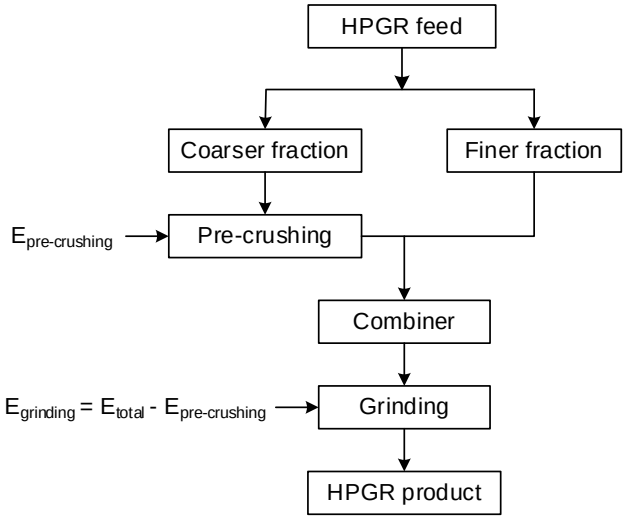

Figure 19 – Schematic of the simulation model

The simulation model has the following three parameters:

1. Critical size, x_c, which is used to classify the HPGR feed into coarse and fine fractions.
2. Energy split, β_{split}, which is used determine energy split between pre-crushing and grinding stages.
3. Constant, c, which is used to multiply by percentage fines, P_{fines}, in equation 11.

The simulation model was fitted using the results of 36 HPGR tests on five different ores. The definition of fines (P_{fines}) varied from 0.355 mm to 2.0 mm. The following model parameters gave good simulation results for all five ore types:

1. x_c =16 mm as the critical size for classifying HPGR feed into to coarser and finer fractions.
2. β_{split} = 0.157 as the constant to split energy between pre-crushing and grinding stages.
3. c = 1.08 as the multiplying constant in equation 11, while P_{fines} defined as percentage passing 1.4 mm in the feed to the grinding stage.

Figure 20 compares the measured and simulation predicted P_{50} and P_{80} for the 36 HPGR tests. The standard error for the P_{50} and the P_{80} are 0.374 mm and 0.485 mm, respectively. The predictions are very good considering that less than 10 kg sample is required for piston press testing to characterize the ores.

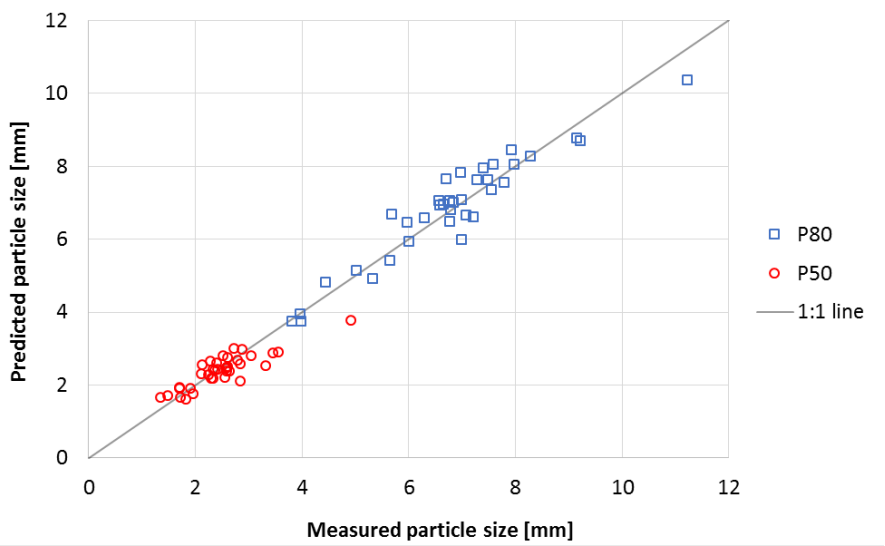

Figure 20 – Simulation results of 36 HPGR tests

Determining Optimal Specific Energy Input

The advantage of the simulation-based methodology is that it can be run at several specific energy levels and the resulting product PSD can be predicted. Figure 21 presents the results of simulation run at specific energy increments of 0.2 kWh/t up to 5 kWh/t to predict the percentage passing 4 mm in the product. It is clear that the percentage passing 4 mm in the HPGR product begins to reach a plateau above 2 kWh/t. One way to optimize the specific energy consumption is to target a specified percentage passing 4 mm in the product. According to Figure 21, simulation of an energy input of 5 kWh/t indicates that the percentage passing 4 mm can reach 71.4%. The Figure 21 shows that the percentage passing 4 mm can reach 57.1% with a specific energy of only 1.33 kWh/t. The simulation results provide valuable HPGR operating information to inform operation of the range where there is clearly diminishing return on the increased energy input.

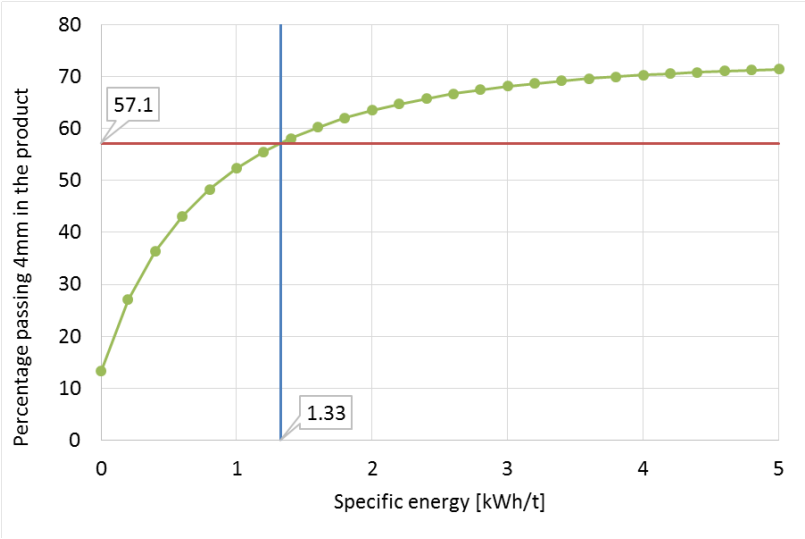

Figure 21 – Percentage passing 4 mm in product versus specific energy plot for a copper/gold ore

Summary of the Simulation Methodology

The simulation methodology can be summarized as having the following four steps:

1. Conduct piston press tests on particles in narrow size fractions.
2. Define the energy–breakage relationship for the ore by determining parameters, M, f^*_{mat}, and n.
3. Define the t_{10}–t_n relationship for the ore or use the set of master curves.
4. Simulate the energy–size reduction performance of the HPGR.

When the HPGR test data is available it is possible to refine the calibration of the simulation model for a specific ore type. Otherwise the three simulation model parameters remain unchanged. The critical size, x_c is 16 mm, energy split constant β_{split} is 0.157, and the multiplying constant c is 1.08 with fines in the feed to grinding stage is defined as percentage passing 1.4 mm.

CONCLUSIONS

Three piston press test procedures were developed:

1. The direct calibration methodology uses around 1000 kg of composite sample and less than 10 kg of sample for predicting the energy-size reduction relationship for varying ore types. Thus, the overall sample requirements are considerably reduced when compared to pilot test programs and the methodology can be used for scoping and feasibility level studies.
2. The database-calibrated methodology requires only 10 kg sample and it provides energy prediction within ±25%, which is acceptable at scoping level studies.
3. The simulation methodology provides a means of simulating closed-circuit operation of the HPGR and is applicable to all stages of metallurgical studies. The methodology can be used for operations to optimize their specific energy consumption and avoid operating in ranges of diminishing return.

Piston press testing procedures significantly reduce the sample requirement as compared to pilot scale test programs that are presently used for sizing and selecting the HPGR. In addition, the piston press tests can be carried out at any facility with a hydraulic press, which are routinely used in rock mechanics and materials testing laboratories (MTS machines). The use of a common hydraulic press makes the piston press test far more accessible than pilot-scale HPGR test facilities that are a few in number and vendor specific.

The three methodologies have generated results that predict the energy size reduction relationship with good levels of accuracy in relation to pilot scale HPGR testing. While pilot results are considered to produce results that are directly scaleable to large HPGR units, the methodologies presented in this paper need to be tested against full scale HPGR operating data.

REFERENCES

Anguelov, R., Ghaffari, H., & Alexander, J. (2008). High Pressure Grinding Rolls (HPGR): an alternative technology versus SAG milling. Presented at the MEI Comminution 2008, Cornwall, England.

Daniel, M. J., Lane, G., & McLean, E. (2010). Efficiency, Economics, Energy and Emissions-Emerging Criteria for Comminution Circuit Decision Making. Presented at the XXV International Mineral Processing Congress, Brisbane, Australia.

Ghaffari, H., Anguelov, R., & Alexander, J. (2013). High Pressure Grinding Rolls (HPGR) in Comparison to SAG Milling Technology. Presented at the 23rd World Mining Congress, Montreal, QC, Canada.

Lim, I. L., Voigt, W., & Weller, K. R. (1996). Product size distribution and energy expenditure in grinding minerals and ores in high pressure rolls. *International Journal of Mineral Processing*, *44-45*, 539–559. http://doi.org/10.1016/0301-7516(95)00064-X

Morrell, S., Lim, W., Shi, F., & Tondo, L. (1997). Modelling of the HPGR crusher. In S. K. Kawatra (Ed.), *Comminution Practices*.

Norgate, T. E., & Weller, K. R. (1994). Selection and operation of high pressure grinding rolls circuits for minimum energy consumption. *Minerals Engineering*, *7*(10), 1253–1267. http://doi.org/10.1016/0892-6875(94)90116-3

Oestreicher, C., & Spollen, C. F. (2006). HPGR versus SAG mill selection for the Los Broncos grinding circuit expansion (Vol. IV, pp. 110–123). Presented at the SAG 2006, Vancouver, BC, Canada.

Parker, B., Rowe, P., Lane, G., & Morrell, S. (2001). The decision to opt for high-pressure grinding rolls for the Boddington expansion (Vol. III, pp. 93–106). Presented at the SAG 2011, Vancouver, BC, Canada.

Rosario, P. (2011). *Comminution Circuit Design and Simulation for the Development of a Novel High Pressure Grinding Roll Circuit* (Ph.D.). The University of British Columbia, Vancouver, BC, Canada.

Shi, F., & Kojovic, T. (2007). Validation of a model for impact breakage incorporating particle size effect. *International Journal of Mineral Processing*, *82*(3), 156–163. http://doi.org/10.1016/j.minpro.2006.09.006

Vanderbeek, J. L., Linde, T. B., Brack, W. S., & Marsden, J. O. (2006). HPGR Implementation at Cerro Verde. In M. J. Allan, K. Major, B. C. Flintoff, B. Klein, & A. L. Mular (Eds.), *International Autogenous and Semiautogenous Grinding Technology 2006* (Vol. IV). Vancouver, BC, Canada.

Wang, C. (2013). *Comparison of HPGR - Ball Mill and HPGR - Stirred Mill Circuits to the Existing AG/SAG Mill - Ball Mill Circuits* (MASc). The University of British Columbia, Vancouver, BC, Canada.